

Mottness Collapse and T-linear Resistivity in Cuprate Superconductors

BY PHILIP PHILLIPS

Department of Physics, University of Illinois 1110 W. Green Street, Urbana, IL 61801, U.S.A.

Central to the normal state of cuprate high-temperature superconductors is the collapse of the pseudogap, briefly reviewed here, at a critical point and the subsequent onset of the strange-metal characterized by a resistivity that scales linearly with temperature. A possible clue to the resolution of this problem is the inter-relation between two facts: 1) A robust theory of T-linear resistivity resulting from quantum criticality requires an additional length scale outside the standard 1-parameter scaling scenario and 2) breaking the Landau correspondence between the Fermi gas and an interacting system with short-range repulsions requires non-fermionic degrees. We show that a low-energy theory of the Hubbard model which correctly incorporates dynamical spectral weight transfer has the extra degrees of freedom needed to describe this physics. The degrees of freedom that mix into the lower band as a result of dynamical spectral weight transfer are shown to either decouple beyond a critical doping, thereby signaling Mottness collapse or unbind above a critical temperature yielding strange metal behaviour characterised by T -linear resistivity.

Keywords: Mottness, superconductivity, strange metal, pseudogap

1. Introduction

High-temperature superconductivity in the copper-oxide ceramics remains an unsolved problem because we do not know what the propagating degrees of freedom are in the normal state. Consequently, we cannot say with any certainty what are the weakly interacting degrees of freedom that pair up to form the superconducting condensate. In low-temperature superconductivity in metals, the existence of a Fermi surface simplified the identification of the propagating degrees of freedom. As shown by Polchinski(Polchinski, 1992), Shankar(Shankar, 1994) and others(Benfatto & Gallavotti, 1990), all renormalizations arising from short-range repulsive interactions are towards the Fermi surface. As a result, such interactions can effectively be integrated out leaving behind dressed electrons or quasiparticles as the propagating degrees of freedom.

Undoped, the cuprates are Mott insulators. Charge localization obtains in Mott systems, not because the band is full, and in fact it is not, but because strong local electron correlations dynamically generate a charge gap by splintering the half-filled band in two. Hence, unlike low-temperature superconductors which are metals in which the (short-range repulsive) interactions are irrelevant, Mott insulation obtains from strong coupling physics. Precisely how the strong correlations

mediate the myriad of phases in the doped cuprates remains unsettled. Nonetheless, there are some experimental facts which are clear. For example, when Mott insulators are doped, a ‘gap’ still remains (Alloul *et al.*, 1989) in the normal state. Dubbed the pseudogap, as zero-energy states exist (Norman *et al.*, 1998) at some momenta, in particular along the diagonal connecting $(0,0)$ and (π,π) , this phenomenon remains one of the most nettling problems in cuprate phenomenology as many of the articles in this volume attest. A typical value for the maximum of the gap along the $(\pi,0)$ direction in underdoped $\text{Bi}_2\text{Sr}_2\text{CaCu}_2\text{O}_{8+\delta}$ (Bi2212) is approximately 45meV at an estimated hole content of 0.1 (Hufner *et al.*, 2008). This hole-content level was obtained, not by counting the number of dopant atoms, as in the case of $\text{La}_{1-x}\text{Sr}_x\text{CuO}_2$ (LSCO), in which the number of doped holes is obtained by counting the number of strontium atoms, but through the empirical formula (Presland *et al.*, 1991)

$$1 - \frac{T_c}{T_c^{\text{max}}} = 82.6(x - 0.16)^2 \quad (1.1)$$

which accurately describes the evolution of the superconducting transition temperature, T_c , for LSCO as a function of doping. While this formula is on firm experimental footing for LSCO, it has been widely criticised in the context of cuprates such as $\text{YBa}_2\text{Cu}_3\text{O}_{7-\delta}$ (Y123) and $\text{Tl}_2\text{Ba}_2\text{CuO}_{6+\delta}$ (Tl2201) in which it is the oxygen content that determines the doping level. For example, Tokura and colleagues (Tokura *et al.*, 1988) and Tutsch, *et al.* (Tutsch *et al.*, 1999) find optimal doping values of $x = 0.21$ and $x = 0.24$, respectively for YBCO. Others (Merz *et al.*, 1998a; Drechsler *et al.*, 1997; Markiewicz & Kusko, 2002) have reached similar conclusions. Hardy and collaborators (Liang *et al.*, 2006) have investigated the validity of Eq. (1.1) for Y123. However, their work does not offer an independent check on the validity of Eq. (1.1) for Y123 because in correlating the change in the c-axis lattice constant (see caption to Fig. 2 (Liang *et al.*, 2006)) with the doping level, they used Eq. (1.1). Consequently, they must confirm that $p_{\text{opt}} = 0.16$ as they report.

I have digressed here on the doping level in the cuprates because one of the key issues with the pseudogap is where precisely it terminates as articulated in the review by Norman, Pines and Kallin (Norman *et al.*, 2005). If the superconducting regions of all the cuprates are artificially made to have optimal doping at a hole content of 0.16, then the pseudogap, as determined (Hufner *et al.*, 2008) by spectroscopic probes such as angle-resolved photoemission (ARPES), scanning tunneling microscopy, and Raman scattering, will terminate at the end of the dome. While not all probes (Ando *et al.*, 2004a; Taillefer, 2009) find that $T^*(x)$ merges with the terminus of the superconducting dome, the problem is partially one of accurately determining the doping level in the cuprates. Luckily, Honma and Hor (Honma & Hor, 2008) have recently addressed the problem of how to determine the doping level unambiguously in the cuprates in which it is the oxygens that act as the dopants. They have advocated (Honma & Hor, 2008) that because the room temperature thermopower data for *all* the cuprates collapses onto a single curve, that curve can be used to calibrate the doping level and hence map out the superconducting region as a function of doping in an unbiased fashion. I reprint here a figure (see Fig. (1)) from their paper which illustrates that the thermopower scale is in excellent agreement with the doping level in Y123 determined by three different experimental methods. With this scale, the optimal doping level for most of the cuprates,

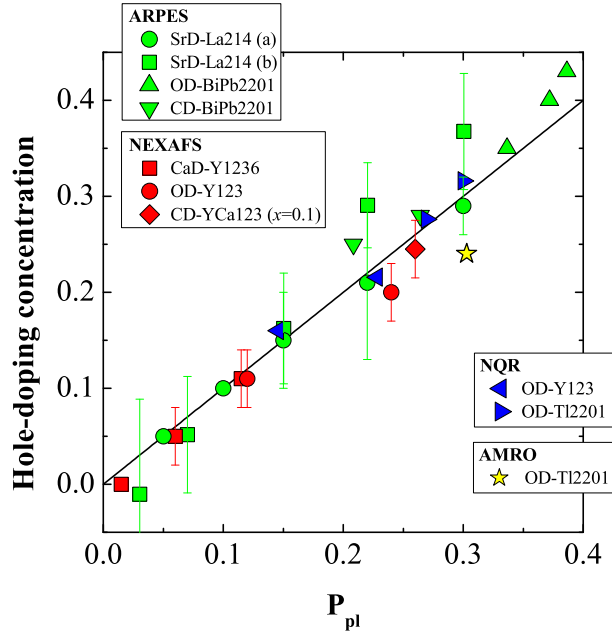


Figure 1. Hole-doping level from various techniques compared with the doping scale extracted from the thermopower, P_{pl} . The red points are obtained from (near-edge X-ray absorption fine structure) NEXAFS: red circles are OD-Y123(Merz *et al.*, 1998b), red diamonds are co-doped Ca-YaC123 (at $x=0.1$)(Merz *et al.*, 1998b), red squares are Calcium-doped Y1236(Merz *et al.*, 1998b). The blue points are from nuclear-quadrupole resonance (NQR) measurements: left blue arrow is OD-Y123(Kotegawa *et al.*, 2001) and the right blue arrow is OD-Ti2201(Kotegawa *et al.*, 2001). The green points are from ARPES: green circles are Strontium-doped La214(Ino *et al.*, 2002), green squares are also Strontium-doped La214(Yoshida *et al.*, 2006b), up arrow, overdoped BiPb2201(Kondo *et al.*, 2005), down arrow co-doped BiP2201(Kondo *et al.*, 2005). The star corresponds to angular magnetoresistance oscillations (AMRO)(Hussey *et al.*, 2003). Reprinted from Phys. Rev. B **77**, 84520 (2008).

except LSCO, occurs at $p_{opt} \approx 0.21 - 0.23$ (Honma & Hor, 2008). This is roughly the doping level at which the pseudogap closes(Taillefer, 2009) as determined by transport measurements(Ando *et al.*, 2004a). In this article, our focus is primarily transport and hence we consider a phase diagram in which the pseudogap crosses the superconducting dome as shown in Fig. (2). That the superconducting region is depicted with a dome should not be taken literally.

Several questions arise with the pseudogap. Is it simply a remnant of the Mott gap? Is it a precursor to superconductivity? Does it represent a new ordered state? Does it compete with superconductivity? Regardless, of how one answers these questions, the phase diagram makes it abundantly clear that the correct theory of the pseudogap should above a characteristic scale, T^* , explain the strange metal in which the resistivity scales linearly with temperature. It is indeed odd then that the

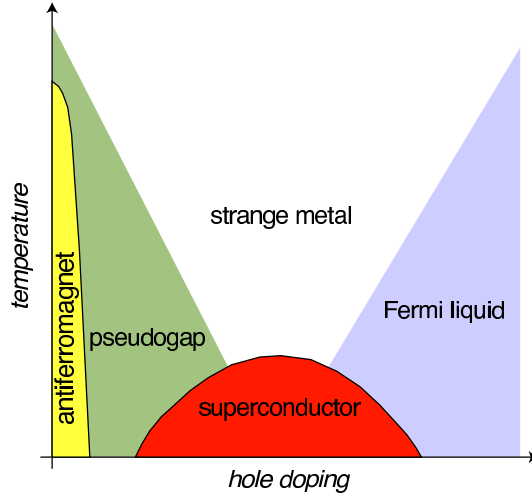


Figure 2. Heuristic phase diagram of the copper-oxide superconductors. In the strange metal, the resistivity is a linear function of temperature. In the pseudogap the single-particle density of states is suppressed without the onset of global phase coherence indicative of superconductivity. As discussed in the introduction, the dome-shape of the superconducting region with an optimal doping level of $x_{\text{opt}} \approx 0.17$ is not quantitatively accurate any cuprate other than LSCO.

plethora of models (Kivelson *et al.*, 1998; Chakravarty *et al.*, 2001; Anderson, 1987; Randeria *et al.*, 1992; Ranninger *et al.*, 1995; Franz & Tešanović, 2001) proposed to explain pseudogap behaviour have had little to say about the strange metal as a robust phenomenon persisting to high temperatures. Part of the problem is that a series of associated phenomena, for example, incipient diamagnetism (Xu *et al.*, 2000) indicative of incoherent pairing (Randeria *et al.*, 1992; Ranninger *et al.*, 1995; Franz & Tešanović, 2001), electronic inhomogeneity (Kivelson *et al.*, 1998; Tranquada *et al.*, 2004; Zaanen & Gunnarsson, 1989; Abbamonte *et al.*, 2005; Pasupathy *et al.*, 2008; Machida, 1989), time-reversal symmetry breaking (Xia *et al.*, 2008; Simon & Varma, 2002; Kaminski *et al.*, 2002; Fauque *et al.*, 2006), and quantum oscillations (Doiron-Leyraud *et al.*, 2007) in the Hall conductivity, possibly associated with the emergence of closed electron (not hole) pockets in the first Brillouin zone (FBZ), are all consistent with some type of order with no immediate connection with the strange metal. We review briefly some of the proposals for the pseudogap, identify the problems in constructing a theory of the strange metal and sketch a possible resolution of this problem based on our recent work involving the exact integration of the high-energy scale in the Hubbard model (Choy *et al.*, 2008*b,a*; Phillips *et al.*, 2009*a*; Leigh & Phillips, 2008; Phillips *et al.*, 2009*b*).

2. Pseudogap Phenomena

The phenomena surrounding the pseudogap (Alloul *et al.*, 1989; Timusk & Statt, 1999; Norman *et al.*, 1998) in the cuprates used to be fairly simple. In zero magnetic field, lightly doped cuprates possess Fermi arcs (Norman *et al.*, 1998) in the normal state. That is, the Fermi surface which is present in the overdoped, more conventional Fermi liquid regime is destroyed on underdoping leaving behind only

a Fermi arc. In actuality, the situation is much worse. That the arc does not represent a collection of well-defined quasiparticles has been clarified by Kanigel, et al. (Kanigel *et al.*, 2006) who showed that in $\text{Bi}_2\text{Sr}_2\text{CaCu}_2\text{O}_{8-\delta}$, the length of the Fermi arc shrinks to zero as T/T^* tends to zero. Consequently, the only remnant of the arc at $T = 0$ is a quasiparticle in the vicinity of $(\pi/2, \pi/2)$ and hence the consistency with nodal metal phenomenology (Balents *et al.*, 1999). Aside from ARPES (Kanigel *et al.*, 2006), Raman data (Le Tacon *et al.*, 2006) also support the nodal/antinodal dichotomy in the underdoped regime.

Recently, however, new ingredients have been added to the pseudogap story in the underdoped regime which, on the surface, are difficult to reconcile with Fermi arcs. At high magnetic fields, quantum oscillations, indicative of a closed Fermi surface, have been observed (Taillefer, 2009) in Y123 and Tl-2201 through measurements of the Hall resistivity, Shubnikov-de Haas effect, and the magnetization in a de Haas-van Alphen experiment. In underdoped samples, the Hall coefficient is negative indicating closed electron-like orbits. Hence, there is an obvious incompatibility, though some have advocated none occurs (Taillefer, 2009), in interpreting the quantum oscillation experiments as a zero-field property of the underdoped cuprates where Fermi arcs obtain. Further, the fields, roughly 50T, at which the quantum oscillations are observed are insufficient to kill the large gap that exists at the antinodal regions. The recent proposal by Pereg-Barnea, et al. (Pereg-Barnea *et al.*, 2010) which shows that quantum oscillations can arise from Fermi arcs terminated by a pairing gap is noteworthy since it points to a possible resolution of the two phenomena.

Also attracting much attention is the recent experimental evidence for nematic order (Daou *et al.*, 2009; Haug *et al.*, 2009). Daou, et al. (Daou *et al.*, 2009) observed that the Nernst signal in Y123 exhibits a large in-plane anisotropy that increases with decreasing temperature. The onset temperature is roughly $T/T^* \approx 0.8$. While the Nernst signal (Xu *et al.*, 2000) had been measured previously (Xu *et al.*, 2000), interpreted as evidence for incoherent pair formation above T_c but not all the way to T^* , it had not been measured with temperature gradients parallel to the a and b axes separately. While nematic order (Kivelson *et al.*, 1998) can give rise to an anisotropy in the Nernst signal, Y123, in the doping regime measured, is already anisotropic in the a - b plane as it is orthorhombic. Further, it has been known for quite some time (Howson *et al.*, 1990) that the thermopower has different signs parallel and perpendicular to the chains in Y123. As the Nernst signal involves the thermopower, such a sign difference could drastically amplify any modest anisotropy that exists among the combination of transport coefficients that contribute to the Nernst signal. Consequently, further experiments are needed to disentangle the inherent a/b axis asymmetry in Y123 from that arising from an electronic phase that spontaneously breaks rotational symmetry.

Theoretical proposals for the pseudogap fall into three groups: 1) Mott-related physics having nothing to do with order (Stanescu & Kotliar, 2006; Anderson, 1987; Phillips, 2010), 2) precursor superconductivity (Randeria *et al.*, 1992; Ranninger *et al.*, 1995; Franz & Tešanović, 2001; Senthil & Lee, 2009), and 3) ordered states that break some type of symmetry, be it 4-fold rotational symmetry (Kivelson *et al.*, 1998), translational symmetry (Tranquada *et al.*, 2004; Chakravarty *et al.*, 2001), or time-reversal symmetry (Kaminski *et al.*, 2002). In fact, experimental data support (Daou *et al.*, 2009; Xia *et al.*, 2008; Simon & Varma, 2002; Haug *et al.*, 2009) many of the or-

dered states proposed for the onset of the pseudogap. However, it is unclear how any of these proposals are related to the origin of the strange metal. Nonetheless, a common approach (Phillips & Chamon, 2005) to meld ordered states with T -linear resistivity is to invoke quantum criticality. However, in its simplest one-parameter form, quantum criticality fails (Phillips & Chamon, 2005) to yield T -linear resistivity unless the dynamical critical exponent is negative, thereby violating causality. This result follows from three simple assumptions: 1) the charges are critical, 2) one-parameter scaling is valid, and 3) the $U(1)$ charge is conserved. These three assumptions yield immediately to a general scaling form for the conductivity

$$\sigma(\omega = 0) = \frac{Q^2}{\hbar} \Sigma(0) \left(\frac{k_B T}{\hbar c} \right)^{(d-2)/z} \quad (2.1)$$

with Q the charge, $\Sigma(0)$ the conductivity at $\omega/T = 0$, and z is the dynamical exponent. As a result, quantum criticality in its present form yields T -linear resistivity (for $d=3$) only if the dynamical exponent satisfies the unphysical constraint $z < 0$. The remedy here might be three-fold: 1) some other yet-unknown phenomenon is responsible for T -linear resistivity, 2) the charge carriers are non-critical, or 3) the single-parameter scaling hypothesis must be relaxed.

Marginal Fermi liquid theory (Varma *et al.*, 1989) (MFL) does, however, offer a phenomenological account of T -linear resistivity. The key point (Varma *et al.*, 1989) here is that at $T = 0$, regardless of momentum, the single-particle scattering rate is proportional to $|\omega|$. Because of the linear dependence of the scattering rate on frequency, MFL phenomenology yields immediately T -linear resistivity. However, at present, there is no microscopic derivation of this highly successful account. Recently, however, the gauge/gravity duality (Maldacena, 1998) has proved useful (Faulkner *et al.*, 2009) in this context. The key claim of the gauge/gravity duality is that some interacting quantum theories at strong coupling in d -space-time dimensions are dual to gravity theories in $d + 1$ dimensional asymptotically anti-de Sitter (AdS_{d+1}) space-time. Unlike the standard equivalence between partition functions for d -dimensional quantum and $d + 1$ -dimensional classical systems in which the extra dimension represents time, in the gauge/gravity duality, the extra dimension represents the renormalization group (RG) scale. That is, in the AdS_{d+1} construction, an infinite number of copies of the original quantum mechanical theory, each at a different RG scale, fill the extra dimension. Hence, the original strongly coupled theory lives entirely at the boundary of the AdS_{d+1} space. In this construction, finite temperature and finite density correspond to having a charged black hole in the bulk geometry. Since the gravity theory is purely classical, all questions surrounding the strong-coupling physics in the original problem can be obtained from solving a set of linear wave equations in the charged black-hole geometry. Using the AdS_4 construction, Liu, McGreevy, and Vegh (Faulkner *et al.*, 2009) computed the single-particle electron spectral function and showed that a range of non-Fermi liquid self-energies can emerge including that of marginal Fermi liquid theory. This result is truly remarkable as it represents the only derivation, albeit not microscopic, of marginal Fermi liquid theory. However, a key question remains. Liu, McGreevy and Vegh (Faulkner *et al.*, 2009) worked entirely with the gravity theory, and hence the underlying quantum theory is not known. Nonetheless, some hints as to the nature of the underlying theory are contained in the gravity solution to marginal Fermi liquid theory. A key feature of the quantum theory on the charged

AdS₄ geometry is that the IR or low-frequency analytic structure of the correlation functions for the charge degrees of freedom are determined entirely by the near horizon metric AdS₂ $\times \mathbb{R}^2$. This serves to illustrate that the degrees of freedom which emerge in the IR and govern the analytic structure of the theory have no correspondence to those in the original UV charged AdS₄ limit. Perhaps the same is true of the underlying microscopic quantum theory which ultimately describes marginal Fermi liquid theory. This suggests that extracting marginal Fermi liquid behaviour from the basic model for a doped Mott insulator might be tricky because the natural variables which would expose this behaviour are not the bare electrons. Within the Hubbard model, it is dynamical spectral weight transfer across the Mott gap that makes the construction of a low-energy theory difficult. Isolating the propagating degrees of freedom which make the low-energy physics weakly interacting amounts to choosing a set of variables which essentially gets rid of the dynamical mixing. Such variables should in principle hold the key to T -linear resistivity. It is precisely this problem that we now address.

3. Fermi Liquid Theory Breakdown: Dynamical Spectral Weight Transfer

To isolate how dynamical spectral weight transfer leads to a breakdown of Fermi liquid theory, it suffices to focus on how the intensity of the band in which the chemical potential resides scales with doping. For hole doping, the relevant band is the lower Hubbard band (LHB). The intensity of a band is equal to the number of charges that can fit into that band. A problem arises for a Fermi liquid account whenever there is a mismatch between the intensity of a band and the number of electrons that can fill the band. Such is the case in the Hubbard model close to half-filling. In the atomic limit, everything is known exactly. There are two bands split by the on-site repulsion U . When x holes are introduced, the intensity of the LHB is $1 + x$ and that of the upper Hubbard band (UHB) is $1 - x$. The weight in the LHB separates into two parts. Since each hole leaves an empty site that can be occupied by either a spin-up or a spin-down electron, the empty part of the LHB has weight $2x$ (Meinders *et al.*, 1993) and the occupied part an intensity of $1 - x$. Hence, we see that the weight of the UHB and the occupied part of the LHB are equal in the atomic limit. This follows from the simple fact that removal of a doubly occupied site also removes one state from the LHB as well. There are, however, t/U corrections to these intensities beyond the atomic limit. In 1967, Harris and Lange (Harris & Lange, 1967) showed that the intensity of the LHB

$$m_{\text{LHB}} = 1 + x + \frac{2t}{U} \sum_{ij\sigma} g_{ij} \langle f_{i\sigma}^\dagger f_{j\sigma} \rangle + \dots = 1 + x + \alpha, \quad (3.1)$$

has t/U corrections (Harris & Lange, 1967) which are entirely positive. Here $f_{i\sigma}$ is related to the original bare fermion operators via a canonical transformation that brings the Hubbard model into block diagonal form in which the energy of each block is nU . In fact, all orders of perturbation theory (Eskes *et al.*, 1994; Harris & Lange, 1967) increase the intensity of the LHB beyond its atomic limit of $1 + x$. It is these dynamical corrections that α denotes. While the intensity of the LHB increases away from the atomic limit, the total number of ways of assigning

electrons to the LHB still remains fixed at $1 + x$. That is, the number of electron states in the LHB is independent of the hopping. Consequently, there is a mismatch between the intensity of the LHB and the number of electrons this band can hold. Since $m_{\text{LHB}} > 1 + x$, additional non-fermionic degrees of freedom are needed to exhaust the phase space of the LHB. These degrees of freedom affect the physics at all energy scales in the LHB. This has a profound consequence. The conserved charge is still the electron filling, n_e which is obtained by integrating the density of states in the LHB up to the chemical potential, appropriately defined. But this quantity now has two contributions,

$$n_e = n_{\text{qp}} + n_{\text{nf}}, \quad (3.2)$$

one coming from the fermionic low-energy degrees of freedom, n_{qp} , in the LHB and the non-fermionic part. As a result, the fermionic quasiparticles in the LHB and the bare electrons can no longer correspond one-to-one as $n_e > n_{\text{qp}}$. This constitutes a breakdown of Fermi liquid theory.

We propose that the chemical potential for the effective number of low-energy fermionic degrees of freedom can be determined by partitioning the spectrum in the LHB so that dynamical spectral weight transfer is essentially removed. In such a picture, the empty part of the spectrum per spin is equal to the weight removed from the occupied part of the LHB when a hole is created. Hence, we arrive at the assignments of the spectral weights in Fig. (3b) in which the doping level is renormalized by the dynamics; that is, $x' = x + \alpha$. That is, the effective number of fermionic degrees of freedom in the LHB is less than the conserved charge. This result already follows from the fact that if the intensity of the LHB exceeds $1 + x$, electrons alone cannot exhaust the total degrees of freedom at low energies. Hence, by Eq. (3.2), there are two contributions to the conserved charge, thereby implying that the number of fermionic quasiparticles is less than the conserved charge. In other words, the dynamical degrees of freedom denoted by α serve to supplement the effective phase space of a hole-doped system and $x' = x + \alpha$ now denotes the effective number of hole degrees of freedom per spin at low energy.

For sufficiently large doping levels, the UHB collapses and the standard weakly interacting picture emerges. At this point, it is no longer meaningful to expand around the atomic limit and the analysis leading to Fig. (3b) fails. This failure arises because, the non-interacting ground state is not adiabatically connected to the atomic limit. Rather, perturbation theory around the band limit should be performed. In this limit, the weight of the band in which the chemical potential resides is 2, completely independent of doping. Hence, there must be a critical point as a function of doping or interaction strength at which the intensity of the lower band jumps to 2. This constitutes a collapse of Mottness. We have advocated (Phillips *et al.*, 2009b) that the doping level at which the UHB collapses coincides with the closing of the pseudogap. This is physically reasonable because unless a gap exists, there is no real separation between the UHB and LHB. The simulations of Kyung, et al. (Kyung *et al.*, 2006) on the Hubbard model also provide clear evidence that a strong correlation exists between the pseudogap and the separation of the low and high energy bands. Experimental evidence for this collapse has been reported recently by Peets, et al. (Peets *et al.*, 2009) from soft x-ray scattering on the oxygen K-edge. In such an experiment, an electron is promoted from the core 1s to an unoccupied level. The experimental observable is the fluo-

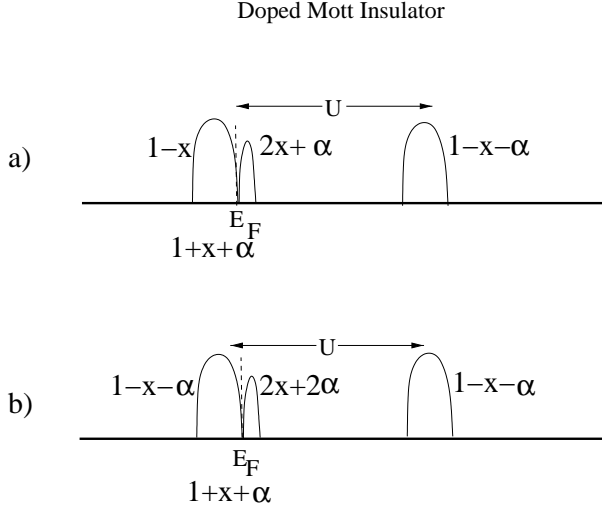


Figure 3. Redistribution of spectral weight in the Hubbard model upon doping the insulating state with x holes. α is the dynamical correction mediated by the doubly occupied sector. To order t/U , this correction worked out by Harris and Lange (Harris & Lange, 1967). a) The traditional approach (Meinders *et al.*, 1993; Hybertsen *et al.*, 1992) in which the occupied part of the lower band is fixed to the electron filling $1-x$. b) New assignment of the spectral weight in terms of dynamically generated charge carriers. In this picture, the weight of the empty part of the LHB per spin is the effective doping level, $x' = x + \alpha$.

rescence yield as a function of energy as electrons relax back to the valence states. Experimentally (Peets *et al.*, 2009), the fluorescence yield is related to the empty part of the spectrum projected onto the oxygen p-orbitals. Consequently, within a 1-band Hubbard model, the relevant quantity is

$$L = \int_{\mu}^{\Lambda} N(\omega) d\omega. \quad (3.3)$$

As shown in Fig. (4), beyond a critical doping level, the slope of the oxygen K-edge intensity changes abruptly. Peets, et al. (Peets *et al.*, 2009) interpreted the slope change as evidence for a saturation and hence a deviation from what is expected in the 1-band Hubbard model. However, given the error bars on the data and the additional point at $x = 0.34$ of Chen, et al. (Chen *et al.*, 1992), one cannot rule out that the data are simply associated with a slope change around a doping level of $x = 0.22$. To verify this assertion, we plotted (Fig. (4)) a computation of L (solid line) by A. Liebsch (Liebsch, 2010) on the 2-d Hubbard model using a self-consistent cluster method. As is evident, the agreement with the solid curve and most of the data points is excellent. Hence, over the complete doping range of interest, the low-energy spectral weight in the cuprates is well described by the doping-induced states in the 1-band Hubbard model.

To summarize, dynamical spectral weight has two profound effects in the normal state of a doped Mott insulator. As long as it is present, a low-energy theory with electrons alone cannot exhaust the total number of charge degrees of freedom in the LHB. This results in a mismatch between the number of fermionic quasiparticles and bare electrons, thereby leading to a breakdown of Fermi liquid theory.

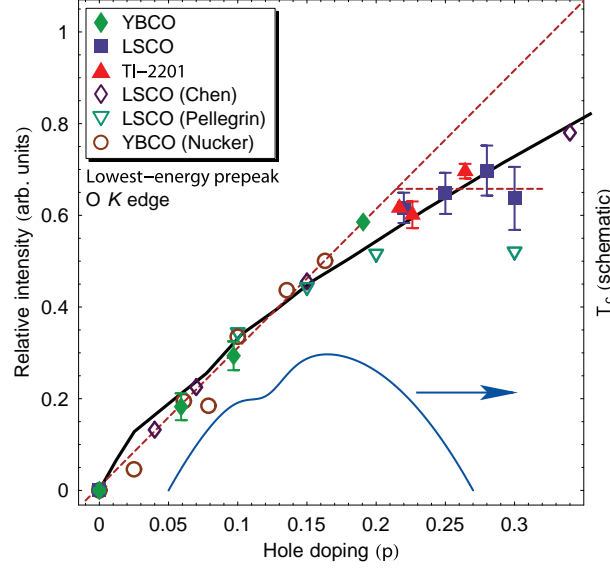


Figure 4. Reprinted from Phys. Rev. Lett. **103**, 087402 (2009). Compilation of the doping dependence of the lowest-energy oxygen K-edge pre-peak from four data sources. The solid plotting symbols are from Peets, et al., (Peets *et al.*, 2009). The open diamonds are taken from Chen, et al. (Chen *et al.*, 1992), open triangles from Pellegrin, et al. (Pellegrin *et al.*, 1993) and open circles from Nücker, et al. (Nücker *et al.*, 1995). The solid straight line is the low-energy spectrum in the Hubbard model computed by A. Liebsch (Liebsch, 2010). A constant scale factor was used to collapse the Liebsch points onto the experimental data since the units of experimental data are arbitrary. The superconducting dome is indicated for reference.

In addition, $L/n_h > 1$ implies that the number of ways of adding particles at low energies exceeds the number of electrons that can be added to the LHB. Consequently, $L/n_h > 1$ is an indication that some states at low energy are gapped to the addition of an electron. Within the experimental accuracy (Peets *et al.*, 2009), there is a dramatic slope change from in L in the vicinity of where the pseudogap closes, adding credence to the emphasis placed here on dynamical spectral weight transfer as the signature of the pseudogap. However, to be completely consistent with the opening of a pseudogap, dynamical spectral weight transfer should also be temperature dependent. We show here that this is the case. Namely, the dynamical correction turns on only below a characteristic temperature set by T^* . This is an indication that some type of bound state formation underlies $\alpha \neq 0$. Above T^* , the new degrees of freedom are unbound and create the T -linear resistivity. Since this mechanism is capable of generating T -linear resistivity beyond T^* and a pseudogap below, we arrive at a consistent theory of two of the most elusive characteristics of the normal state of the cuprates.

4. Low-energy Theory of Motttness

In the parameter space relevant to the cuprates, the Hubbard model represents strongly coupled physics. In this regime, no continuum limit exists and as a consequence, no firm statement can be made as to the precise nature of the charge

carriers. Ultimately, it is only correct in this regime to focus on the current, which can be given an interpretation in terms of single-particles if the propagating degrees of freedom can be identified. Such an identification should be possible once the high-energy scale is correctly integrated out. A successful low-energy reduction of the Hubbard model should reveal the new degree of freedom that causes the intensity of the lower band to exceed $1 + x$. As this degree of freedom arises from the mixing with the doubly occupied sites, it should have charge $2e$. Charge $2e$ objects do not contribute to the fluorescence yield of the single-particle spectrum unless they combine with something else to produce a charge e entity. The proposed mechanism for the pseudogap is ‘doublon-holon’ bound-state formation mediated by a collective IR charge $2e$ mode. Below a characteristic temperature, such bound states are stable. Quite generally, such bound states are expected to mediate the Mott insulating state as well. Consider half-filling. Even in the half-filled state, the dynamical mixing that leads to a non-zero α is still present. That is, double occupancy is present even in the ground state of a half-filled band. Since a doubly occupied site must result in the simultaneous creation of an empty site, the insulating state persists only if the doubly occupied and empty site are bound as has been proposed previously (Castellani *et al.*, 1979; Kohn, 1964; Mott, 1949). Else, hole conduction obtains.

Such binding should emerge from the correct low-energy theory of a half-filled Hubbard band. We have shown previously (Leigh *et al.*, 2007; Choy *et al.*, 2008*b,a*; Phillips *et al.*, 2009*a*; Leigh & Phillips, 2008; Phillips, 2010), how the high-energy degrees of freedom can be integrated out exactly at any filling. The key idea is (Leigh *et al.*, 2007; Choy *et al.*, 2008*a*; Phillips *et al.*, 2009*a*; Leigh & Phillips, 2008) to extend the Hilbert space by introducing a new fermionic field that creates excitations on the U scale without identifying such physics with double occupancy. At half-filling the Lagrangian (Leigh & Phillips, 2008) simplifies to

$$L_{\text{IR}}^{\text{hf}} = 2 \frac{|s|^2}{U} |\varphi_\omega|^2 + 2 \frac{|\tilde{s}|^2}{U} |\tilde{\varphi}_\omega|^2 + \frac{t^2}{U} |b_\omega|^2 \quad (4.1)$$

$$+ s \gamma_{\mathbf{p}}^{(\mathbf{k})}(\omega) \varphi_{\omega, \mathbf{k}}^\dagger c_{\mathbf{k}/2+\mathbf{p}, \omega/2+\omega', \uparrow} c_{\mathbf{k}/2-\mathbf{p}, \omega/2-\omega', \downarrow} \\ + \tilde{s}^* \tilde{\gamma}_{\mathbf{p}}^{(\mathbf{k})}(\omega) \tilde{\varphi}_{-\omega, \mathbf{k}} c_{\mathbf{k}/2+\mathbf{p}, \omega/2+\omega', \uparrow} c_{\mathbf{k}/2-\mathbf{p}, \omega/2-\omega', \downarrow} + h.c., \quad (4.2)$$

This theory contains two bosonic fields with charge $2e$ (φ^\dagger) and $-2e$ ($\tilde{\varphi}$). These bosonic modes are collective degrees of freedom, not made out of the elemental excitations, which represent dynamical mixing with U -scale physics, namely, the contribution of double holes ($-2e$) and double occupancy ($2e$) to any state of the system. Here s and \tilde{s} are constants with units of energy, all operators in Eq. (4.1) have the same site index, repeated indices are summed both over the site index and frequency, ω , $c_{i\sigma}^\dagger$ creates a fermion on site i with spin σ ,

$$b_{\mathbf{k}} = \sum_{\mathbf{p}} \varepsilon_{\mathbf{p}}^{(\mathbf{k})} c_{\mathbf{k}/2+\mathbf{p}, \uparrow} c_{\mathbf{k}/2-\mathbf{p}, \downarrow}, \quad (4.3)$$

and the dispersion is given by $\varepsilon_{\mathbf{p}}^{(\mathbf{k})} = 4 \sum_{\mu} \cos(k_{\mu}a/2) \cos(p_{\mu}a)$, where \mathbf{k} and \mathbf{p} are

the center of mass and relative momenta of the fermion pair. The coefficients

$$\begin{aligned}\gamma_{\mathbf{p}}^{(\mathbf{k})}(\omega) &= \frac{-U + t\varepsilon_{\mathbf{p}}^{(\mathbf{k})} + 2\omega}{U} \sqrt{1 + 2\omega/U} \\ \tilde{\gamma}_{\mathbf{p}}^{(\mathbf{k})}(\omega) &= \frac{U + t\varepsilon_{\mathbf{p}}^{(\mathbf{k})} + 2\omega}{U} \sqrt{1 - 2\omega/U}\end{aligned}\quad (4.4)$$

play a special role in this theory as they account for the turn-on of the spectral weight. At the level of a Lagrangian, the vanishing of the coefficient of a quadratic term defines the dispersion of the associated particle. All the terms which are naively quadratic, Eq. (4.1), possess constant coefficients and hence we reach the conclusion that there are no propagating bosons or electrons. What Eq. (4.1) lays plain is that the turn-on of the spectral weight in a Mott insulator cannot be formulated in terms of bare electrons, at least in a low-energy theory. This is consistent with the emerging view (Dzyaloshinskii, 2003; Essler & Tsvelik, 2002; Rosch, 2007) that in a Mott insulator, the single-particle Green function vanishes along a locus of points in momentum space. Physically, a vanishing of the single-particle electron Green function implies that the electrons are not the propagating degrees of freedom. Precisely what the propagating degrees of freedom are is determined by the dispersing modes in the low-energy Lagrangian. Consider the second line of the Lagrangian, Eq. (4.2). Appearing here are two interaction terms, which describe composite excitations, whose coefficients can vanish. Fig. (5b) shows explicitly that the vanishing of γ and $\tilde{\gamma}$ leads to spectral weight which is strongly peaked at two distinct energies, $\pm U/2$. Each state in momentum space has spectral weight at these two energies. The width of the bands is $8t$. The particles which give rise to the turn-on of the spectral weight are composite excitations or the bound states of the bosonic and fermionic degrees of freedom determined by the interaction terms $\varphi^\dagger cc$ and $\tilde{\varphi} cc$. In the terms of the variables appearing in the Hubbard model, we make the heuristic association of the composite excitations with bound states of double occupancy and holes as has been postulated previously (Castellani *et al.*, 1979) to be the ultimate source of the gap in a Mott insulator. This association is entirely heuristic because the variables the variables in the original UV In so far as they generate the spectral weight, the interaction terms can be thought of as the kinetic terms in the low-energy action. The gap (Mott gap) in the spectrum for the composite excitations obtains for $U > 8t$ as each band is centered at $\pm U/2$ with a width of $8t$. Fig. (5) demonstrates that the transition to the Mott insulating state found here proceeds by a discontinuous vanishing of the spectral weight at the chemical potential to zero but a continuous evolution of the Mott gap as is seen in numerical calculations (Park *et al.*, 2008) in finite-dimensional lattices but not in the $d = \infty$ (Georges *et al.*, 1996) solution.

In terms of the bare electrons, the overlap with the composite excitations determines the Mott gap. To determine the overlap, it is tempting to complete the square on the $\varphi^\dagger cc$ term bringing it into a quadratic form, $\Psi^\dagger \Psi$ with $\Psi = A\varphi + Bcc$. This would lead to composite excitations having charge $2e$, a vanishing of the overlap and hence no electron spectral density of any kind. However, the actual excitations that underlie the operator $\varphi^\dagger cc$ correspond to a linear combination of charge e objects, c^\dagger and $\varphi^\dagger c$. In terms of the UV variables, the latter can be thought of as a doubly occupied site bound to a hole. At half-filling (Choy *et al.*, 2008b; Phillips *et al.*,

2009a), the exact representation of the electron creation

$$\begin{aligned} c_{i,\sigma}^\dagger \rightarrow \tilde{c}_{i,\sigma}^\dagger &\equiv -V_\sigma \frac{t}{U} \left(c_{i,-\sigma} b_i^\dagger + b_i^\dagger c_{i,-\sigma} \right) \\ &+ V_\sigma \frac{2}{U} \left(s\varphi_i^\dagger + \tilde{s}\tilde{\varphi}_i \right) c_{i,-\sigma} \end{aligned} \quad (4.5)$$

is indeed a sum of two composite excitations, the first having to do with spin fluctuations ($b^\dagger c$) and the other with high-energy physics, $\varphi^\dagger c$ and $\tilde{\varphi}c$, that is, excitations in the UHB and LHB, respectively. We can think of the overlap

$$O = |\langle c^\dagger | \tilde{c}^\dagger \rangle \langle \tilde{c}^\dagger | \Psi^\dagger \rangle|^2 P_\Psi \quad (4.6)$$

in terms of the physical process of passing an electron through a Mott insulator. The overlap will involve that between the bare electron with the low-energy excitations of Eq. (4.5), $\langle c | \tilde{c} \rangle$, and the overlap with the propagating degrees of freedom, $\langle \tilde{c} | \Psi \rangle$ with P_Ψ , the propagator for the composite excitations. Because of the dependence on the bosonic fields in Eq. (4.5), O retains destructive interference between states above and below the chemical potential. Such destructive interference between excitations across the chemical potential leads to a vanishing of the spectral weight at low energies (Meinders *et al.*, 1993). Consequently, the turn-on of the *electron* spectral weight cannot be viewed simply as a sum of the spectral weight for the composite excitations. As a result of the destructive interference, the gap in the electron spectrum will always exceed that for the composite excitations. Hence, establishing (Fig. (5)) that the composite excitations display a gap is a sufficient condition for the existence of a charge gap in the electron spectrum. A simple calculation (Leigh & Phillips, 2008), Fig. (5c), of the electron spectral function at $U = 8t$ confirms this basic principle that a gap in the propagating degrees of freedom guarantees that the electron spectrum is gapped. Further, Fig. (5) confirms that the electron spectral function involves interference across the Mott scale. Consequently, although the composite excitations are sharp, corresponding to poles in a propagator as in Eq. (4.2), the electrons are not.

(a) Binding-Unbinding Transition

The bound states that mediate the Mott gap also survive in the doped state. In fact, through dynamical spectral weight transfer, such bound states are transferred down in energy from the UHB. That some type of bound state must exist in the doped state of a Mott insulator can be inferred from the work of Gor'kov and Teitel'baum (Gor'kov & Teitel'baum, 2006). They observed remarkably that the charge carrier concentration, n_{Hall} , extracted from the inverse of the Hall coefficient in $\text{La}_{2-x}\text{Sr}_x\text{CuO}_4$ (LSCO) obeys an empirical formula,

$$n_{\text{Hall}}(x, T) = n_0(x) + n_1(x) \exp(-\Delta(x)/T), \quad (4.7)$$

appropriate for a two-component or two-fluid system. One of the components is independent of temperature, $n_0(x)$ (x the doping level) while the other is strongly temperature dependent, $n_1(x) \exp(-\Delta(x)/T)$. The key observation here is that the temperature dependence in n_{Hall} is carried entirely within $\Delta(x, T)$ which defines a characteristic activation energy scale for the system, the pseudogap scale. Hence, a

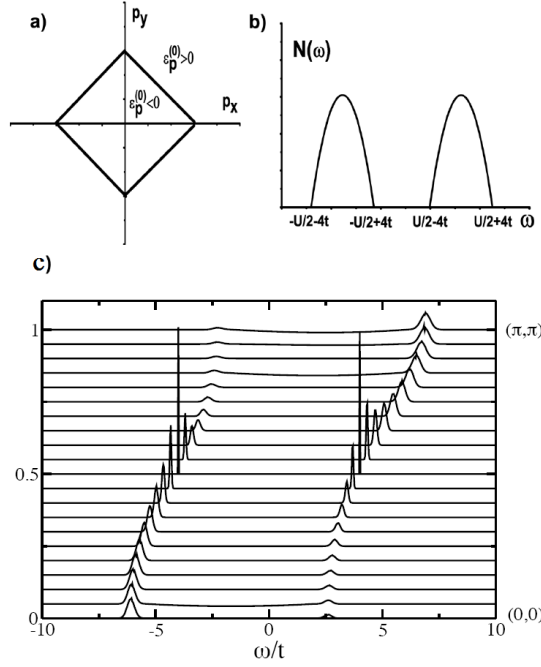


Figure 5. a) Diamond-shaped surface in momentum space where the particle dispersion changes sign. b) Turn-on of the spectral weight in the upper and lower Hubbard bands for the composite excitations as a function of energy and momentum. In the UHB of the composite excitations, the spectral density is determined to $\gamma_{\mathbf{p}}$ while for the LHB it is governed by $\tilde{\gamma}_{\mathbf{p}}$. The corresponding operators which describe the turn-on of the spectral weight are the composite excitations $\varphi^{\dagger}cc$ (UHB) and $\tilde{\varphi}cc$ (LHB).

charge density that obeys Eq. (4.7) is symptomatic of a gap in the spectrum. Eq. (4.7) offers direct confirmation for a renormalization of the doping level purely from dynamical effects. Our key contention here is that α arises from the second term in Eq. (4.7) and is mediated by the binding of φ_i^{\dagger} to a hole.

We computed the Hall coefficient (Chakraborty & Phillips, 2009) in this theory by first obtaining the spectral function. As the computation of the spectral function is instructive in unclocking the new propagating degrees of freedom, we recount it here. Noting that the conserved charge is given by

$$Q = \sum_i c_{i\sigma}^{\dagger} c_{i\sigma} + 2 \sum_i \varphi_i^{\dagger} \varphi_i, \quad (4.8)$$

the spectral function for just the fermionic component at low energies $c_{i\sigma}$ will necessarily have an integrated weight less than $1 - x$ (Chakraborty *et al.*, 2009). To illustrate this, we treat φ_i initially as a spatially independent field, owing to the lack of any gradient terms of φ_i in the action. Note, that the integrated weight of the UHB is less than $1 - x$ follows strictly from the form of the conserved charge not from any approximation scheme that is used to compute the spectral function.

The electron Green function is then written as a path integral over the φ fields as

$$G(\mathbf{k}, \omega) = \frac{1}{Z} \int [D\varphi^*][D\varphi] FT \left(\int [dc_i^*][dc_i] c_i(t) c_i^*(0) \right) \times \exp \left(- \int L(c, \varphi) dt \right) \quad (4.9)$$

where the effective Lagrangian L is expressed in a diagonalized form

$$L = \sum_{k\sigma} \gamma_{k\sigma}^* \dot{\gamma}_{k\sigma} + \sum_k (E_0 + E_k - \lambda_k) + \sum_{k\sigma} \lambda_k \gamma_k^* \gamma_k, \quad (4.10)$$

where the $\gamma_{k\sigma}$ are the Bogoliubov quasiparticles and are given by

$$\gamma_{k\uparrow}^* = \cos \theta_k c_{k\uparrow}^* + \sin \theta_k c_{-k\downarrow} \quad (4.11)$$

$$\gamma_{k\downarrow} = -\sin \theta_k c_{k\uparrow}^* + \cos \theta_k c_{-k\downarrow} \quad (4.12)$$

where $\cos^2 \theta_k = \frac{1}{2} (1 + \frac{E_k}{\lambda_k})$, $\alpha_k = 2(\cos k_x + \cos k_y)$, $E_0 = (-2\mu + \frac{s^2}{U})\varphi^* \varphi$, $E_k = -g_t t \alpha_k - \mu$, $\lambda_k = \sqrt{E_k^2 + \Delta_k^2}$, the gap is proportional to s , $\Delta_k = s\varphi^*(1 - \frac{2t}{U}\alpha_k)$, and hence vanishes when φ is absent and $g_t = \frac{2\delta}{1+\delta}$, $\delta = 1-n$. The g_t term originates from the correlated hopping term, $(1 - n_{i\bar{\sigma}})c_{i\sigma}^\dagger c_{j\sigma}(1 - n_{j\bar{\sigma}})$. The $\gamma_{k\sigma}$'s play the role of the fundamental low energy degrees of freedom in a doped Mott insulator. That is, they are the natural propagating charge degrees of freedom. Note they depend in a complicated way on the φ_i field and consequently are heavily mixed with the doubly occupied sector. Upon integrating out the fermions, we obtain,

$$G(k, \omega) = \frac{1}{Z} \int [D\varphi^*][D\varphi] G(k, \omega, \varphi) \exp^{-\sum_k (E_0 + E_k - \lambda_k - \frac{2}{\beta} \ln(1 + e^{-\beta \lambda_k}))} \quad (4.13)$$

where

$$G(k, \omega, \varphi) = \frac{\sin^2 \theta_k [\varphi]}{\omega + \lambda_k [\varphi]} + \frac{\cos^2 \theta_k [\varphi]}{\omega - \lambda_k [\varphi]} \quad (4.14)$$

is the exact Green function corresponding to the Lagrangian, Eq. (4.10), which has a two-branch structure, corresponding to the bare electrons and the coupled holon-doublon state respectively. The role of the φ field, which determines the weight of the second branch, is vital to our understanding of the properties of Mott systems, as was demonstrated previously (Choy *et al.*, 2008b; Phillips *et al.*, 2009a,b). It is trivial to see that in the limit of vanishing s (no φ field), the $\gamma_{k\sigma}$'s reduce to the bare electron operators c_k and the first term in Eq. (4.14) vanishes. The two-fluid nature of the response stems from this fact of the theory. Namely, the first term contributes only when $\varphi \neq 0$ and the second when $\varphi = 0$ as depicted in the spectral function in Fig. (6a). These contributions correspond to the dynamical and static components of the spectral weight, respectively and appear as two distinct branches in the electron spectral function. Since the second branch corresponds to a bound degree of freedom, a gap opens at the chemical potential. As we demonstrate in

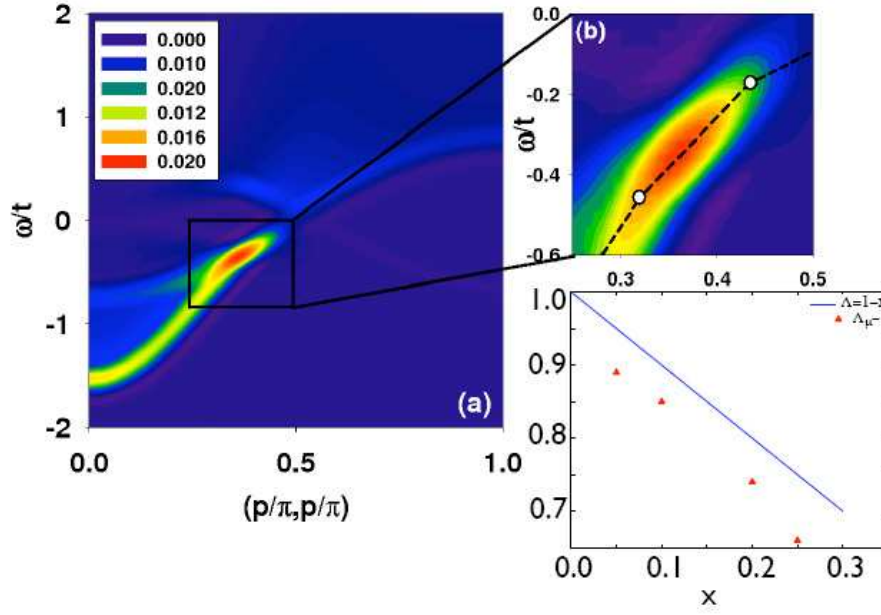


Figure 6. (a) Spectral function for filling $n = 0.9$ along the nodal direction. The intensity is indicated by the color scheme. (b) Location of the low and high energy kinks as indicated by the change in the slope of the electron dispersion. (c) Integrated weight (triangles) of the fermionic part of the spectral function. The deviation from $1 - x$ (straight line) stems from the form of the conserved charge in Eq. (4.8).

Fig. (6c), the total weight of both branches which composes the total number of fermionic degrees of freedom is less than the conserved charge $1 - x$. This is dictated by the fact that conserved charge at low energies, Eq. (4.8), consists of a fermionic as well as a bosonic component, thereby directly supporting the partitioning of the spectral weight in Fig. (3b).

We obtained the Green function $G(\mathbf{k}, \omega)$ by numerical integration and the subsequent spectral function, $A(\mathbf{k}, \omega)$. We computed the Hall coefficient from the spectral function using

$$R_H = \sigma_{xy} / \sigma_{xx}^2, \quad (4.15)$$

where

$$\begin{aligned} \sigma_{xy} &= \frac{2\pi^2 |e|^3 aB}{3\hbar^2} \int d\omega \left(\frac{\partial f(\omega)}{\partial \omega} \right) \frac{1}{N} \sum_{\mathbf{k}} \left(\frac{\partial \epsilon_{\mathbf{k}}}{\partial k_x} \right)^2 \\ &\times \frac{\partial^2 \epsilon_{\mathbf{k}}}{\partial k_y^2} A(\mathbf{k}, \omega)^3 \end{aligned} \quad (4.16)$$

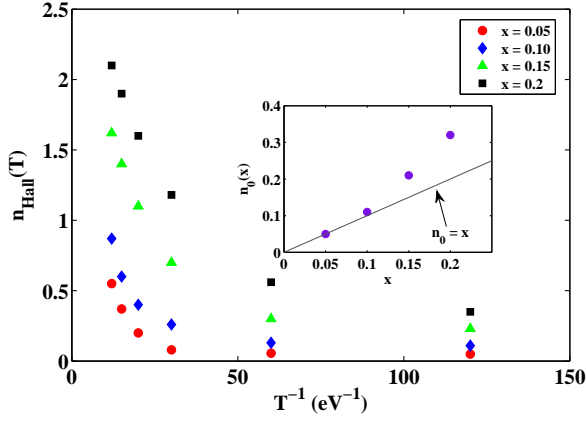


Figure 7. n_{Hall} plotted as a function of inverse temperature for four different values of hole doping x : 1) solid circles, $x = 0.05$, 2) diamonds, $x = 0.10$, 3) triangles, $x = 0.15$, and 4) squares, $x = 0.2$. The inset shows the temperature independent part of the carrier density as a function of x . Note it exceeds the nominal doping level indicated by the straight line.

and

$$\sigma_{xx} = \frac{\pi e^2}{2\hbar a} \int d\omega \left(-\frac{\partial f(\omega)}{\partial \omega} \right) \frac{1}{N} \sum_{\mathbf{k}} \left(\frac{\partial \epsilon_{\mathbf{k}}}{\partial k_x} \right)^2 A(\mathbf{k}, \omega)^2 \quad (4.17)$$

with σ_{xx} and σ_{xy} the diagonal and off-diagonal components of the conductivity tensor respectively, $f(\omega)$ is the Fermi distribution function, and B is the normal component of the external magnetic field. The effective charge carrier density n_{Hall} is then obtained using the relation $R_H = -1/(n_{\text{Hall}}e)$. Fig.7 shows a set of plots of n_{Hall} as a function of the inverse temperature, each corresponding to a different value of hole-doping, x , in the underdoped regime (x ranging from 0.05 to 0.20). The plots fit remarkably well to an exponentially decaying form. In other words, the computed charge carrier density within the charge $2e$ boson theory of a doped Mott insulator agrees well with the form given in Eq. (4.7) proposed by Gor'kov and Teitel'baum (Gor'kov & Teitel'baum, 2006). The inset shows the temperature-independent part of the charge density as a function of x . This quantity exceeds the nominal doping level (Yoshida *et al.*, 2006a). Such a deviation the nominal doping level is also supported by angle-resolved photoemission spectroscopy (ARPES). Shown in Fig. (9) is a plot of the measured Fermi surface, x_{FS} in LSCO as a function of the nominal doping level x . As is clear, x_{FS} deviates from linearity precisely where our calculated value of $n_0(x)$ does. In fact, the agreement between the inset in Fig. (7) and Fig. (9) is striking. Nonetheless, in previous publications (Yoshida *et al.*, 2006a), this deviation was attributed to a band dispersion effect. The clear corroboration of this effect with our strong-coupling calculation suggests that the ultimate source of the deviation from linearity is Mottness. In a hole-doped Mott insulator, the Hall coefficient must change sign (Takagi *et al.*, 1989) before the particle-hole symmetric condition for the atomic limit, namely when $2x = 1 - x$ or equivalently before $x = 1/3$ (Stanescu & Phillips, 2004; Shastry *et al.*, 1993).

The ‘binding energy’, $\Delta(x)$, was extracted for each doping and plotted in Fig.(8) using Eq. (4.7). Shown here also are the values for the experimentally determined

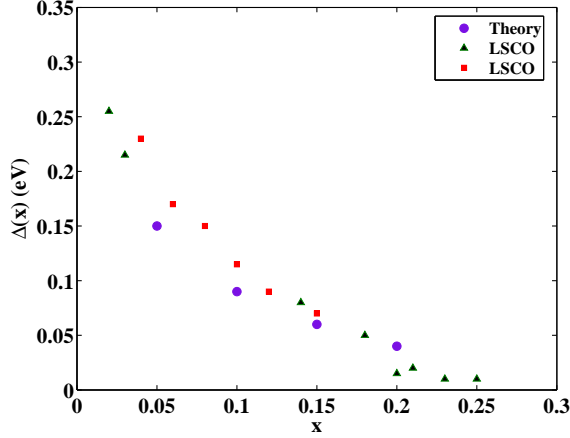


Figure 8. $\Delta(x)$ (solid circles) obtained from fitting the plots in Fig.(7) to Eq.(4.7) plotted as a function of hole doping x . The experimental values are also shown for LSCO: solid triangles(Ando *et al.*, 2004b; Ono *et al.*, 2007; Padilla *et al.*, 2005) and squares(Nishikawa *et al.*, 1994) The excellent agreement indicates that the bound component contributing to the charge density does in fact give rise to the pseudogap.

pseudogap energy for LSCO(Ando *et al.*, 2004b; Ono *et al.*, 2007; Padilla *et al.*, 2005). The magnitude of $\Delta(x)$ falls with increasing hole doping as is seen experimentally and hence is consistent with its interpretation, even quantitatively, as a measure of the pseudogap temperature T^* . A rough estimate of T^* ,

$$T^*(x) \approx -\Delta(x)/\ln(x), \quad (4.18)$$

may be obtained from $\Delta(x)$, by equating the number of doped carriers x with that of the activated ones $n_1(x)\exp(-\Delta(x, T))$ as proposed by Gor'kov and Teitel'baum(Gor'kov & Teitel'baum, 2006). Fig.(10) shows a plot of T^* as a function of x . This result is in qualitative agreement with the experimentally obtained estimates of T^* (Timusk & Statt, 1999; Yoshizaki *et al.*, 1990; Nakano *et al.*, 1994).

(b) *T-linear Resistivity*

The physical picture for the charge $2e$ boson calculation is now clear. Below a characteristic temperature the boson is bound to a hole and produces charge e states. This leads to a non-zero value for α . Above, T^* , the bound states break up. The simplest way of understanding why the charge $2e$ boson must be bound at low energies, aside from the fact that it has no bare dynamics, is that once the high-energy sector is integrated out exactly, the Hilbert space shrinks back to the Fock space of the Hubbard model.

The mechanism for T -linear resistivity is simple within this model. Once the binding energy of the boson vanishes, bosons are free to scatter off the electrons. The absence of a kinetic energy term for the bosons implies that their dynamics are classical. The resistivity of electrons scattering off classical bosons is well-known to scale linearly with temperature above the energy to create the boson as depicted in Fig. (11). Hence, this mechanism is robust and should persist to high temperatures. Consequently, the charge $2e$ boson reduction of the Hubbard model offers

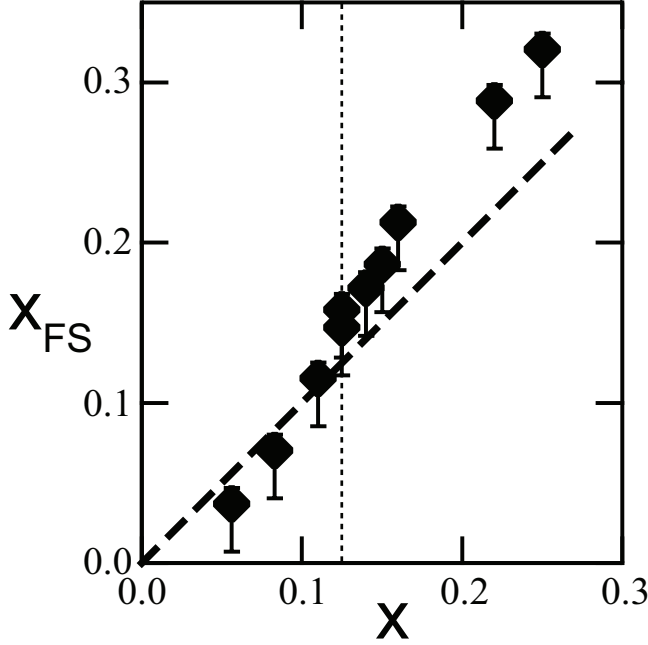


Figure 9. Measured Fermi surface from ARPES (extracted from [http://arxiv: 0911.2245](http://arxiv.org/abs/0911.2245)) plotted versus the nominal doping level. The deviation from linearity is corroborated by Fig. (8) thereby signifying that strong coupling physics is the root cause.

a resolution of the pseudogap and the transition to the strange metal regime of the cuprates. Further, the mechanism for the strange metal is consistent with the scaling analysis leading to Eq. (2.1). Namely, T -linear resistivity requires an additional energy scale absent from a single-parameter scaling analysis. In the exact low-energy theory, a charge $2e$ boson emerges as a new degree of freedom. While it is bound in the pseudogap regime, its unbinding beyond a critical temperature or doping provides the added degree of freedom to generate the anomalous temperature dependence for the resistivity. A further experimental prediction of this work then is that the strange metal regime should be populated with charge $2e$ excitations, without the usual diamagnetic signal. Shot noise measurements are ideally suited for testing this prediction.

5. Final Remarks

We have focused here on explaining three inter-related facts. F1) Breaking the Landau correspondence between the Fermi gas and the interacting system requires new degrees of freedom. F2) The connection between T -linear resistivity and quantum criticality is only possible if an additional degree of freedom outside the one-parameter paradigm is present as Eq. (2.1) lays plain. F3) The total weight of the low-energy band exceeds the number of ways electrons can be assigned to this band, thereby requiring new low-energy degrees of freedom. The common ingredient among F1-F3 is a new degree of freedom distinct from the electrons. Explicitly carrying out the Wilsonian program for the Hubbard model by integrating out the

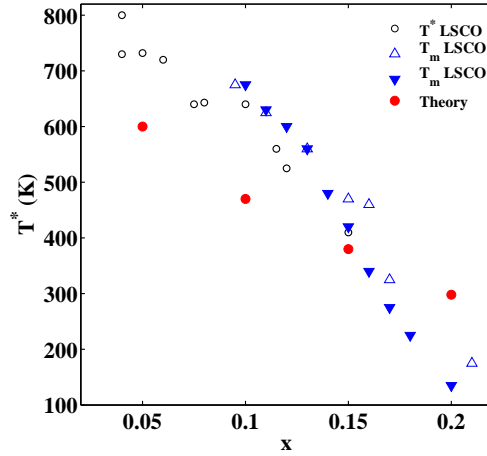


Figure 10. $T^*(x)$ (solid circles) obtained from Eq.(4.18) plotted as a function of hole doping x . The experimental data were gleaned from the following: open circles are from Ref.(Timusk & Statt, 1999) T^* , open triangles (T_m) from Ref.(Yoshizaki *et al.*, 1990), and closed triangles (T_m) from Ref.(Nakano *et al.*, 1994).

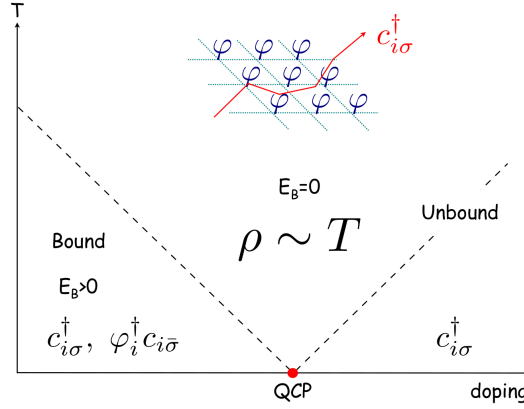


Figure 11. Phase diagram for the dynamics mediated by the charge $2e$ boson, φ_i . Bound states between form between the holes and the charge $2e$ boson as seen in the calculation of the Hall coefficient, giving rise to $E_B > 0$ with E_B the binding energy. The pseudogap regime terminates at a quantum critical point (QCP) where the bosons and holes unbind. In the critical regime, the dominant scattering mechanism is still due to the interaction with the charge $2e$ bosons. In this regime, the energy to excite the bosons vanishes. T-linear resistivity results anytime electrons scatter off classical bosons with $T > \omega_b$, where ω_b is the energy to excite a boson as in the electron-phonon problem above the Debye temperature. To the right of the quantum critical regime, the boson is irrelevant and scattering is dominated by electron-electron interactions indicative of a Fermi liquid.

high-energy sector produces the missing degree of freedom that is capable of explaining all of these facts. Since it is the mixing with the doubly occupied sector that enhances the intensity of the LHB beyond $1+x$, the new degree of freedom at low energies must have charge $2e$ and hence must be bosonic. This has been

explicitly demonstrated by the exact procedure to integrate out the high-energy sector. At low energies and temperatures, the charge $2e$ boson mediates new charge e states in the LHB. Such bound states already exist in the half-filled system and constitute the propagating degrees of freedom that describe the UHB and LHB. Hence, the pseudogap emerges in the charge $2e$ theory as a remnant of the Mott gap. Heuristically, the bound states and hence the gap originate from a doubly occupied site bound to a hole.

This work makes a series of experimental predictions. First, below the T^* line $L/n_h > 1$ whereas above $L/n_h = 1$. This information can be extracted from temperature-dependent experiments of the kind leading to Fig. (4). Second, any experimental probe that couples to the low-energy excitations should be interpreted in terms of x' , not the bare hole number x . These include measurements of the 1) optical conductivity, 2) superfluid density, and 3) ‘fermi surface’ volumes extracted from quantum oscillation experiments (typically Hall measurements). The latter is particularly germane because the Fermi surface volumes extracted experimentally (Doiron-Leyraud *et al.*, 2007; LeBoeuf *et al.*, 2007) for YBCO are not consistent with any integer multiple of the physically doped holes.

That the charge $2e$ boson mediates local bound states is *a priori* expected as it lacks a bare kinetic term. The bound states that form account for the pseudogap and their breakup leads to a resistivity that quite generally scales linearly with temperature. As long as the UHB is present, the program carried out here is sufficient to describe the physics of a doped Mott insulator. Once the UHB collapses, traditional Fermi liquid descriptions obtain. As a separation between the UHB and LHB is only meaningful if there is a gap in the spectrum, the pseudogap lies at the heart of Mottness. Precisely the role such bound states play in the superconducting state remains open.

I thank R. Leigh, T.-P. Choy, S. Hong, S. Chakraborty, D. Galanakis, and S. Chakraborty for extensive collaborations which led to the work summarized here. I also thank Frank Krüger, Lance Cooper and P. Abbamonte for extensive discussions on Mottness. I also acknowledge financial support from the NSF DMR-0940992 and the Center for Emergent Superconductivity, a DoE Energy Frontier Research Center, Award Number DE-AC0298CH1088.

References

- Abbamonte, P., Rusydi, A., Smadici, S., Gu, G. D., Sawatzky, G. A. & Feng, D. L. 2005 Spatially modulated ‘mottness’ in $\text{La}_2\text{-x}\text{Ba}_x\text{CuO}_4$. *Nat Phys*, **1**(3), 155–158.
- Alloul, H., Ohno, T. & Mendels, P. 1989 y_{89} nmr evidence for a fermi-liquid behavior in $y\text{Ba}_2\text{Cu}_3\text{O}_{6+x}$. *Phys. Rev. Lett.*, **63**(16), 1700–1703. (doi:10.1103/PhysRevLett.63.1700)
- Anderson, P. W. 1987 The resonating valence bond state in La_2CuO_4 and superconductivity. *Science*, **235**(4793), 1196–1198.
- Ando, Y., Komiya, S., Segawa, K., Ono, S. & Kurita, Y. 2004*a* Electronic phase diagram of high- T_c cuprate superconductors from a mapping of the in-plane resistivity curvature. *Phys. Rev. Lett.*, **93**(26), 267 001. (doi:10.1103/PhysRevLett.93.267001)
- Ando, Y., Kurita, Y., Komiya, S., Ono, S. & Segawa, K. 2004*b* Evolution of the hall coefficient and the peculiar electronic structure of the cuprate superconductors. *Physical Review Letters*, **92**(19).

- Balents, L., Fisher, M. P. A. & Nayak, C. 1999 Dual order parameter for the nodal liquid. *Physical Review B*, **60**(3).
- Benfatto, G. & Gallavotti, G. 1990 Perturbation theory of the fermi surface in a quantum liquid: A general quasiparticle formalism and one-dimensional systems. *Journal of Statistical Physics*, **959**, 541–664.
- Castellani, C., Castro, C. D., Feinberg, D. & Ranninger, J. 1979 New model hamiltonian for the metal-insulator transition. *Phys. Rev. Lett.*, **43**(26), 1957–1960. (doi:10.1103/PhysRevLett.43.1957)
- Chakraborty, S., Hong, S. & Phillips, P. 2009 Non-conservation of fermionic degrees of freedom in doped mott insulators. *arXiv:0909.2854*.
- Chakraborty, S. & Phillips, P. 2009 Two-fluid model of the pseudogap of high-temperature cuprate superconductors based on charge-2e bosons. *Physical Review B (Condensed Matter and Materials Physics)*, **80**(13), 132505. (doi:10.1103/PhysRevB.80.132505)
- Chakravarty, S., Laughlin, R. B., Morr, D. K. & Nayak, C. 2001 Hidden order in the cuprates. *Phys. Rev. B*, **63**(9), 094503. (doi:10.1103/PhysRevB.63.094503)
- Chen, C. T., Tjeng, L. H., Kwo, J., Kao, H. L., Rudolf, P., Sette, F. & Fleming, R. M. 1992 Out-of-plane orbital characters of intrinsic and doped holes in $La_2 - xSr_xCuO_4$. *Phys. Rev. Lett.*, **68**(16), 2543–2546. (doi:10.1103/PhysRevLett.68.2543)
- Choy, T.-P., Leigh, R. G. & Phillips, P. 2008a Hidden charge-2e boson: Experimental consequences for doped mott insulators. *Physical Review B (Condensed Matter and Materials Physics)*, **77**(10), 104524–9.
- Choy, T.-P., Leigh, R. G., Phillips, P. & Powell, P. D. 2008b Exact integration of the high energy scale in doped mott insulators. *Physical Review B (Condensed Matter and Materials Physics)*, **77**(1), 014512–12.
- Daou, R., Chang, J., LeBoeuf, D., Cyr-Choiniere, O., Laliberte, F., Doiron-Leyraud, N., Ramshaw, B. J., Liang, R., Bonn, D. A. *et al.* 2009 Broken rotational symmetry in the pseudogap phase of a high- T_c superconductor. *arXiv:0909.4430*.
- Doiron-Leyraud, N., Proust, C., LeBoeuf, D., Levallois, J., Bonnemaïson, J.-B., Liang, R., Bonn, D. A., Hardy, W. N. & Taillefer, L. 2007 Quantum oscillations and the fermi surface in an underdoped high- T_c superconductor. *Nature*, **447**(7144), 565–568.
- Drechsler, S. L., Málek, J. & Eschrig, H. 1997 Exact diagonalization study of the hole distribution in CuO_3 chains within the four-band dp model. *Physical Review B*, **55**(1).
- Dzyaloshinskii, I. 2003 Some consequences of the luttinger theorem: The luttinger surfaces in non-fermi liquids and mott insulators. *Phys. Rev. B*, **68**(8), 085113. (doi:10.1103/PhysRevB.68.085113)
- Eskes, H., Oleś, A. M., Meinders, M. B. J. & Stephan, W. 1994 Spectral properties of the hubbard bands. *Phys. Rev. B*, **50**(24), 17980–18002. (doi:10.1103/PhysRevB.50.17980)
- Essler, F. H. L. & Tsvelik, A. M. 2002 Weakly coupled one-dimensional mott insulators. *Phys. Rev. B*, **65**(11), 115117. (doi:10.1103/PhysRevB.65.115117)
- Faulkner, T., Liu, H., McGreevy, J. & Vegh, D. 2009 Emergent quantum criticality, fermi surfaces, and ads_2 . *arXiv:0907.2694*.

- Fauque, B., Sidis, Y., Hinkov, V., Pailhes, S., Lin, C. T., Chaud, X. & Bourges, P. 2006 Magnetic order in the pseudogap phase of high- T_c superconductors. *Physical Review Letters*, **96**(19), 197 001–4.
- Franz, M. & Tešanović, Z. 2001 Algebraic fermi liquid from phase fluctuations: topological fermions, vortex Berry's phase and qcd theory of cuprate superconductors. *Phys. Rev. Lett.*, **87**(25), 257 003. (doi:10.1103/PhysRevLett.87.257003)
- Georges, A., Kotliar, G., Krauth, W. & Rozenberg, M. J. 1996 Dynamical mean-field theory of strongly correlated fermion systems and the limit of infinite dimensions. *Rev. Mod. Phys.*, **68**(1), 13. (doi:10.1103/RevModPhys.68.13)
- Gor'kov, L. P. & Teitelbaum, G. B. 2006 Interplay of externally doped and thermally activated holes in $La_{2-x}Sr_xCuO_4$ and their impact on the pseudogap crossover. *Physical Review Letters*, **97**(24), 247 003–4.
- Harris, A. B. & Lange, R. V. 1967 Single-particle excitations in narrow energy bands. *Phys. Rev.*, **157**(2), 295–314. (doi:10.1103/PhysRev.157.295)
- Haug, D., Hinkov, V., Suchanek, A., Inosov, D. S., Christensen, N. B., Niedermayer, C., Bourges, P., Sidis, Y., Park, J. T. *et al.* 2009 Magnetic-field-enhanced incommensurate magnetic order in the underdoped high-temperature superconductor $YBa_2Cu_3O_{6.45}$. *Physical Review Letters*, **103**(1), 017001. (doi:10.1103/PhysRevLett.103.017001)
- Honma, T. & Hor, P. H. 2008 Unified electronic phase diagram for hole-doped high- T_c cuprates. *Physical Review B (Condensed Matter and Materials Physics)*, **77**(18), 184 520–16.
- Howson, M. A., Salamon, M. B., Friedmann, T. A., Rice, J. P. & Ginsberg, D. 1990 Anomalous peak in the thermopower of $YBa_2Cu_3O_{7-\delta}$ single crystals: A possible fluctuation effect. *Physical Review B*, **41**(1).
- Hufner, S., Hossain, M. A., Damascelli, A. & Sawatzky, G. A. 2008 Two gaps make a high-temperature superconductor? *Reports on Progress in Physics*, **71**(6), 062 501 (9pp).
- Hussey, N. E., Abdel-Jawad, M., Carrington, A., Mackenzie, A. P. & Balicas, L. 2003 A coherent three-dimensional fermi surface in a high-transition-temperature superconductor. *Nature*, **425**(6960), 814–817.
- Hybertsen, M. S., Stechel, E. B., Foulkes, W. M. C. & Schlüter, M. 1992 Model for low-energy electronic states probed by x-ray absorption in high- T_c cuprates. *Physical Review B*, **45**(17).
- Ino, A., Kim, C., Nakamura, M., Yoshida, T., Mizokawa, T., Fujimori, A., Shen, Z. X., Kakeshita, T., Eisaki, H. *et al.* 2002 Doping-dependent evolution of the electronic structure of $La_{2-x}Sr_xCuO_4$ in the superconducting and metallic phases. *Physical Review B*, **65**(9).
- Kaminski, A., Rosenkranz, S., Fretwell, H. M., Campuzano, J. C., Li, Z., Raffy, H., Cullen, W. G., You, H., Olson, C. G. *et al.* 2002 Spontaneous breaking of time-reversal symmetry in the pseudogap state of a high- T_c superconductor. *Nature*, **416**(6881), 610–613.
- Kanigel, A., Norman, M. R., Randeria, M., Chatterjee, U., Souma, S., Kaminski, A., Fretwell, H. M., Rosenkranz, S., Shi, M. *et al.* 2006 Evolution of the pseudogap from fermi arcs to the nodal liquid. *Nat Phys*, **2**(7), 447–451.

- Kivelson, S. A., Fradkin, E. & Emery, V. J. 1998 Electronic liquid-crystal phases of a doped mott insulator. *Nature*, **393**(6685), 550–553.
- Kohn, W. 1964 Theory of the insulating state. *Physical Review*, **133**(1A).
- Kondo, T., Takeuchi, T., Mizutani, U., Yokoya, T., Tsuda, S. & Shin, S. 2005 Contribution of electronic structure to thermoelectric power in $(bi, pb)_2(sr, la)_2cuo_6 + \delta$. *Phys. Rev. B*, **72**(2), 024 533. (doi:10.1103/PhysRevB.72.024533)
- Kotegawa, H., Tokunaga, Y., Ishida, K., Zheng, G.-q., Kitaoka, Y., Kito, H., Iyo, A., Tokiwa, K., Watanabe, T. *et al.* 2001 Unusual magnetic and superconducting characteristics in multilayered high- t_c cuprates: 63cu nmr study. *Phys. Rev. B*, **64**(6), 064 515. (doi:10.1103/PhysRevB.64.064515)
- Kyung, B., Kancharla, S. S., S  n  chal, D., Tremblay, A.-M. S., Civelli, M. & Kotliar, G. 2006 Pseudogap induced by short-range spin correlations in a doped mott insulator. *Phys. Rev. B*, **73**(16), 165 114. (doi:10.1103/PhysRevB.73.165114)
- Le Tacon, M., Sacuto, A., Georges, A., Kotliar, G., Gallais, Y., Colson, D. & Forget, A. 2006 Two energy scales and two distinct quasiparticle dynamics in the superconducting state of underdoped cuprates. *Nat Phys*, **2**(8), 537–543.
- LeBoeuf, D., Doiron-Leyraud, N., Levallois, J., Daou, R., Bonnema  son, J. B., Hussey, N. E., Balicas, L., Ramshaw, B. J., Liang, R. *et al.* 2007 Electron pockets in the fermi surface of hole-doped high- t_c superconductors. *Nature*, **450**(7169), 533–536.
- Leigh, R. G. & Phillips, P. 2008 Origin of the mott gap. *arXiv:0812.0593*.
- Leigh, R. G., Phillips, P. & Choy, T.-P. 2007 Hidden charge 2e boson in doped mott insulators. *Physical Review Letters*, **99**(4), 046 404–4.
- Liang, R., Bonn, D. A. & Hardy, W. N. 2006 Evaluation of cuo[sub 2] plane hole doping in yba[sub 2]cu[sub 3]o[sub 6 + x] single crystals. *Physical Review B (Condensed Matter and Materials Physics)*, **73**(18), 180 505–4.
- Liebsch, A. 2010 Spectral weight of doping-induced states in the 2d hubbard model. *arXiv:1004.1322*.
- Machida, K. 1989 Magnetism in la2cuo4 based compounds. *Physica C: Superconductivity*, **158**(1-2), 192–196.
- Maldacena, J. 1998 The large n limit of superconformal field theories and supergravity. *Adv. Theor. Math. Phys.*, **2**, 231–252.
- Markiewicz, R. S. & Kusko, C. 2002 Phase separation models for cuprate stripe arrays. *Physical Review B*, **65**(6).
- Meinders, M. B. J., Eskes, H. & Sawatzky, G. A. 1993 Spectral-weight transfer: Breakdown of low-energy-scale sum rules in correlated systems. *Phys. Rev. B*, **48**(6), 3916–3926. (doi:10.1103/PhysRevB.48.3916)
- Merz, M., N  cker, N., Schweiss, P., Schuppler, S., Chen, C. T., Chakarian, V., Freeland, J., Idzerda, Y. U., Kl  ser, M. *et al.* 1998a Site-specific x-ray absorption spectroscopy of y1-xcaxba2cu3o7-y: Overdoping and role of apical oxygen for high temperature superconductivity. *Physical Review Letters*, **80**(23).

- Merz, M., Nücker, N., Schweiss, P., Schuppler, S., Chen, C. T., Chakarian, V., Freeland, J., Idzerda, Y. U., Kläser, M. *et al.* 1998*b* Site-specific x-ray absorption spectroscopy of $y_{1-x}Ca_{x}Ba_2Cu_3O_{7-y}$: Overdoping and role of apical oxygen for high temperature superconductivity. *Phys. Rev. Lett.*, **80**(23), 5192–5195. (doi:10.1103/PhysRevLett.80.5192)
- Mott, N. F. 1949 The basis of the electron theory of metals, with special reference to the transition metals. *Proceedings of the Physical Society. Section A*, **62**(7), 416–422.
- Nakano, T., Oda, M., Manabe, C., Momono, N., Miura, Y. & Ido, M. 1994 Magnetic properties and electronic conduction of superconducting $La_{2-x}Sr_xCuO_4$. *Phys. Rev. B*, **49**(22), 16 000–16 008. (doi:10.1103/PhysRevB.49.16000)
- Nishikawa, T., Takeda, J. & Sato, M. 1994 Transport anomalies of high- T_c oxides above room temperature. *Journal of the Physical Society of Japan*, **63**(4), 1441–1448.
- Norman, M. R., Ding, H., Randeria, M., Campuzano, J. C., Yokoya, T., Takeuchi, T., Takahashi, T., Mochiku, T., Kadowaki, K. *et al.* 1998 Destruction of the fermi surface in underdoped high- T_c superconductors. *Nature*, **392**(6672), 157–160.
- Norman, M. R., Pines, D. & Kallin, C. 2005 The pseudogap: Friend or foe of high T_c ? *Advances in Physics*, **54**, 715–733.
- Nücker, N., Pellegrin, E., Schweiss, P., Fink, J., Molodtsov, S. L., Simmons, C. T., Kaindl, G., Frentrup, W., Erb, A. *et al.* 1995 Site-specific and doping-dependent electronic structure of $YBa_{2-x}Cu_{3-y}O_{7-x}$ probed by O 1s and Cu 2p x-ray-absorption spectroscopy. *Physical Review B*, **51**(13).
- Ono, S., Komiya, S. & Ando, Y. 2007 Strong charge fluctuations manifested in the high-temperature hall coefficient of high- T_c cuprates. *Physical Review B (Condensed Matter and Materials Physics)*, **75**(2), 024 515–8.
- Padilla, W. J., Lee, Y. S., Dumm, M., Blumberg, G., Ono, S., Segawa, K., Komiya, S., Ando, Y. & Basov, D. N. 2005 Constant effective mass across the phase diagram of high- T_c cuprates. *Phys. Rev. B*, **72**(6), 060 511. (doi:10.1103/PhysRevB.72.060511)
- Park, H., Haule, K. & Kotliar, G. 2008 Cluster dynamical mean field theory of the mott transition. *Physical Review Letters*, **101**(18), 186 403–4.
- Pasupathy, A. N., Pushp, A., Gomes, K. K., Parker, C. V., Wen, J., Xu, Z., Gu, G., Ono, S., Ando, Y. *et al.* 2008 Electronic origin of the inhomogeneous pairing interaction in the high- T_c superconductor $Bi_2Sr_2CaCu_2O_{8+\delta}$. *Science*, **320**(5873), 196–201.
- Peets, D. C., Hawthorn, D. G., Shen, K. M., Kim, Y.-J., Ellis, D. S., Zhang, H., Komiya, S., Ando, Y., Sawatzky, G. A. *et al.* 2009 X-ray absorption spectra reveal the inapplicability of the single-band hubbard model to overdoped cuprate superconductors. *Physical Review Letters*, **103**(8), 087 402–4.
- Pellegrin, E., Nücker, N., Fink, J., Molodtsov, S. L., Gutiérrez, A., Navas, E., Strebel, O., Hu, Z., Domke, M. *et al.* 1993 Orbital character of states at the fermi level in $La_{2-x}Sr_xCuO_4$ and $R_{2-x}Ce_xCuO_4$ ($R=Nd, Sm$). *Physical Review B*, **47**(6).
- Pereg-Barnea, T., Weber, H., Refael, G. & Franz, M. 2010 Quantum oscillations from fermi arcs. *Nat Phys*, **6**(1), 44–49.
- Phillips, P. 2010 Colloquium: Identifying the propagating charge modes in doped mott insulators. *Rev. Mod. Phys.*, **82**(2), 1719–1742. (doi:10.1103/RevModPhys.82.1719)

- Phillips, P. & Chamon, C. 2005 Breakdown of one-parameter scaling in quantum critical scenarios for high-temperature copper-oxide superconductors. *Phys. Rev. Lett.*, **95**(10), 107 002. (doi:10.1103/PhysRevLett.95.107002)
- Phillips, P., Choy, T.-P. & Leigh, R. G. 2009a Motttness in high-temperature copper-oxide superconductors. *Reports on Progress in Physics*, **72**(3), 036 501 (24pp).
- Phillips, P., Choy, T.-P. & Leigh, R. G. 2009b Motttness in high-temperature copper-oxide superconductors. *Reports on Progress in Physics*, **72**(3), 036 501 (24pp).
- Polchinski, J. 1992 Effective field theory and the fermi surface.
- Presland, M. R., Tallon, J. L., Buckley, R. G., Liu, R. S. & Flower, N. E. 1991 General trends in oxygen stoichiometry effects on T_c in Bi and Tl superconductors. *Physica C: Superconductivity*, **176**(1-3), 95–105.
- Randeria, M., Trivedi, N., Moreo, A. & Scalettar, R. T. 1992 Pairing and spin gap in the normal state of short coherence length superconductors. *Phys. Rev. Lett.*, **69**(13), 2001–2004. (doi:10.1103/PhysRevLett.69.2001)
- Ranninger, J., Robin, J. M. & Eschrig, M. 1995 Superfluid precursor effects in a model of hybridized bosons and fermions. *Phys. Rev. Lett.*, **74**(20), 4027–4030. (doi:10.1103/PhysRevLett.74.4027)
- Rosch, A. 2007 Breakdown of Luttinger’s theorem in two-orbital Mott insulators. *The European Physical Journal B*, **59**(4), 495–502. (doi:10.1140/epjb/e2007-00312-3)
- Senthil, T. & Lee, P. A. 2009 Synthesis of the phenomenology of the underdoped cuprates. *Physical Review B (Condensed Matter and Materials Physics)*, **79**(24), 245116. (doi:10.1103/PhysRevB.79.245116)
- Shankar, R. 1994 Renormalization-group approach to interacting fermions. *Rev. Mod. Phys.*, **66**(1), 129–192. (doi:10.1103/RevModPhys.66.129)
- Shastry, B. S., Shraiman, B. I. & Singh, R. R. P. 1993 Faraday rotation and the Hall constant in strongly correlated Fermi systems. *Phys. Rev. Lett.*, **70**(13), 2004–2007. (doi:10.1103/PhysRevLett.70.2004)
- Simon, M. E. & Varma, C. M. 2002 Detection and implications of a time-reversal breaking state in underdoped cuprates. *Phys. Rev. Lett.*, **89**(24), 247 003. (doi:10.1103/PhysRevLett.89.247003)
- Stanescu, T. D. & Kotliar, G. 2006 Fermi arcs and hidden zeros of the Green function in the pseudogap state. *Physical Review B (Condensed Matter and Materials Physics)*, **74**(12), 125110. (doi:10.1103/PhysRevB.74.125110)
- Stanescu, T. D. & Phillips, P. 2004 Nonperturbative approach to full Mott behavior. *Phys. Rev. B*, **69**(24), 245 104. (doi:10.1103/PhysRevB.69.245104)
- Taillefer 2009 Fermi surface reconstruction in high- T_c superconductors. *arXiv:0901.2313*.
- Takagi, H., Ido, T., Ishibashi, S., Uota, M., Uchida, S. & Tokura, Y. 1989 Superconductor-to-nonsuperconductor transition in $(La_{1-x}Sr_x)_{2}CuO_4$ as investigated by transport and magnetic measurements. *Phys. Rev. B*, **40**(4), 2254–2261. (doi:10.1103/PhysRevB.40.2254)

- Timusk, T. & Statt, B. 1999 The pseudogap in high-temperature superconductors: an experimental survey. *Reports on Progress in Physics*, **62**(1), 61–122.
- Tokura, Y., Torrance, J. B., Huang, T. C. & Nazzari, A. I. 1988 Broader perspective on the high-temperature superconducting $\text{YBa}_2\text{Cu}_3\text{O}_y$ system: The real role of the oxygen content. *Physical Review B*, **38**(10).
- Tranquada, J. M., Woo, H., Perring, T. G., Goka, H., Gu, G. D., Xu, G., Fujita, M. & Yamada, K. 2004 Quantum magnetic excitations from stripes in copper oxide superconductors. *Nature*, **429**(6991), 534–538.
- Tutsch, U., Schweiss, P., Hauff, R., Obst, B., Wolf, T. & Wahl, H. 1999 Calorimetric investigation of $\text{NdBa}_2\text{Cu}_3\text{O}_x$ single crystals. *Journal of Low Temperature Physics*, **117**(3), 951–955.
- Varma, C. M., Littlewood, P. B., Schmitt-Rink, S., Abrahams, E. & Ruckenstein, A. E. 1989 Phenomenology of the normal state of Cu-O high-temperature superconductors. *Physical Review Letters*, **63**(18).
- Xia, J., Schemm, E., Deutscher, G., Kivelson, S. A., Bonn, D. A., Hardy, W. N., Liang, R., Siemons, W., Koster, G. *et al.* 2008 Polar Kerr-effect measurements of the high-temperature $\text{YBa}_2\text{Cu}_3\text{O}_{6+x}$ superconductor: Evidence for broken symmetry near the pseudogap temperature. *Physical Review Letters*, **100**(12), 127002. (doi:10.1103/PhysRevLett.100.127002)
- Xu, Z. A., Ong, N. P., Wang, Y., Kakeshita, T. & Uchida, S. 2000 Vortex-like excitations and the onset of superconducting phase fluctuation in underdoped $\text{La}_{2-x}\text{Sr}_x\text{CuO}_4$. *Nature*, **406**(486-488).
- Yoshida, T., Zhou, X. J., Tanaka, K., Yang, W. L., Hussain, Z., Shen, Z.-X., Fujimori, A., Sahrakorpi, S., Lindroos, M. *et al.* 2006a Systematic doping evolution of the underlying Fermi surface of $\text{La}_{2-x}\text{Sr}_x\text{CuO}_4$. *Phys. Rev. B*, **74**(22), 224 510. (doi:10.1103/PhysRevB.74.224510)
- Yoshida, T., Zhou, X. J., Tanaka, K., Yang, W. L., Hussain, Z., Shen, Z.-X., Fujimori, A., Sahrakorpi, S., Lindroos, M. *et al.* 2006b Systematic doping evolution of the underlying Fermi surface of $\text{La}_{2-x}\text{Sr}_x\text{CuO}_4$. *Physical Review B (Condensed Matter and Materials Physics)*, **74**(22), 224510. (doi:10.1103/PhysRevB.74.224510)
- Yoshizaki, R., Ishikawa, N., Sawada, H., Kita, E. & Tasaki, A. 1990 Magnetic susceptibility of normal state and superconductivity of $\text{La}_{2-x}\text{Sr}_x\text{CuO}_4$. *Physica C: Superconductivity*, **166**(5-6), 417 – 422. (doi:DOI:10.1016/0921-4534(90)90038-G)
- Zaanen, J. & Gunnarsson, O. 1989 Charged magnetic domain lines and the magnetism of high- T_c oxides. *Phys. Rev. B*, **40**(10), 7391–7394. (doi:10.1103/PhysRevB.40.7391)